Supporting Information

Interaction of Dicoordinate Phosphorus with Boranes: Chemistry of 3a,6a-Diaza-1,4-diphosphapentalene as Masked Phosphinidene

Yulia S. Panova,[a] Alexandra V. Khristolyubova[a], Natalia V. Zolotareva,[a] Vyacheslav V. Sushev,[a] Vadim E. Galperin,[a] Roman V. Rumyantcev,[a] Georgy K. Fukin,[a] and Alexander N. Kornev*[a]

G. A. Razuvaev Institute of Organometallic Chemistry, Russian Academy of Sciences, 49 Tropinin str., 603137 Nizhny Novgorod, Russia

Table of Contents

Table S1. The crystal data and structures refinement details for complexes **14**, **16**, **17**, and **18**.

Complex	**14**	**16**	**17**	**18**
Empirical formula	$C_{24}H_{26}B_2Cl_4N_2P_2$	$C_{39}H_{25}BF_{15}N_2P_2$	$C_{30}H_{18}BClF_{15}N_2OP_2$ (0.5 CH_2Cl_2)	$C_{24}H_{42}B_4N_4P_4$
Formula Weight	567.83	879.36	822.68	553.73
Crystal System	Orthorhombic	Monoclinic	Triclinic	Monoclinic
Space Group	*Pna2(1)*	*P2(1)/n*	*P-1*	*P2(1)/c*
a, Å	17.2276(5)	9.8192(4)	9.3112(4)	13.6969(5)
b, Å	11.6430(3)	13.9606(6)	11.7738(5)	12.2887(4)
c, Å	12.7160(4)	26.3145(10)	16.1431(6)	18.2101(6)
α, °	90	90	97.5990(10)	90
β, °	90	95.7722(16)	100.6420(10)	110.0090(10)
γ, °	90	90	110.4190(10)	90
V, Å^3	2550.59(13)	3589.0(3)	1592.42(11)	2880.06(17)
Z	4	4	2	4
d_{calc}, Mg/m^3	1.479	1.627	1.716	1.277
μ, mm^{-1}	0.608	0.234	0.341	0.284
F_{000}	1168	1772	822	1176
Crystal Size, mm	0.300 x 0.100 x 0.100	0.100 x 0.070 x 0.030	0.315 x 0.287 x 0.054	0.340 x 0.210 x 0.130
θ Range for Data Collection, °	2.111 - 28.742	2.133 - 26.021	2.058 - 27.999	2.291 - 28.997
Index Ranges	-23 ≤ h ≤ 23 -11 ≤ k ≤ 15 -17 ≤ l ≤ 16	-12 ≤ h ≤ 12 -17 ≤ k ≤ 17 -32 ≤ l ≤ 32	-12 ≤ h ≤ 12 -15 ≤ k ≤ 15 -21 ≤ l ≤ 21	-14 ≤ h ≤ 18 -16 ≤ k ≤ 16 -24 ≤ l ≤ 21
Reflns Collected / unique	26774 / 6456	39748 / 6948	20336 / 7606	28496 / 7616
R_{int}	0.0305	0.0669	0.0342	0.0432
Completeness to θ, %	99.8	98.8	99.7	99.6
Data / restraints / parameters	6456 / 567 / 351	6948 / 93 / 576	7606 / 40 / 522	7616 / 30 / 384
$S(F^2)$	1.047	1.073	1.050	1.032
Final *R* Indices ($I > 2\sigma(I)$)	R_1 = 0.0588 wR_2 = 0.1304	R_1 = 0.0807 wR_2 = 0.1470	R_1 = 0.0467 wR_2 = 0.0960	R_1 = 0.0520 wR_2 = 0.1193
R Indices (all data)	R_1 = 0.0636 wR_2 = 0.1326	R_1 = 0.1188 wR_2 = 0.1601	R_1 = 0.0650 wR_2 = 0.1012	R_1 = 0.0783 wR_2 = 0.1280
Largest Diff. Peak and Hole, e/Å^3	0.566 / -0.632	0.730 / -0.510	0.501 / -0.625	0.711 / -0.429

Table S2. The main topological parameters for the selected bonds and interatomic interactions in **16**.

Bond	ρ(**r**), a.e.	∇^2ρ(**r**), a.e.	*v*(**r**), a.e.	h_e(**r**), a.e.	$\lvert E_{EML}\rvert^*$, Kcal/mol
P(1)-N(1)	0.127	0.188	-0.244	-0.099	76.7
P(2)-N(2)	0.148	0.384	-0.331	-0.117	103.8
N(1)-N(2)	0.344	-0.550	-0.490	-0.314	153.6
B(1)-P(1)	0.089	-0.119	-0.066	-0.048	20.6
P(1)-C(1)	0.160	-0.121	-0.271	-0.151	85.2
N(2)-C(2)	0.274	-0.482	-0.554	-0.337	173.7
C(1)-C(2)	0.327	-0.984	-0.518	-0.382	162.6
C(8)-N(1)	0.304	-0.491	-0.683	-0.403	214.2
C(7)-P(2)	0.175	0.050	-0.346	-0.167	108.6
C(8)-C(7)	0.306	-0.894	-0.445	-0.334	139.7
C(25)-B(1)	0.151	-0.103	-0.242	-0.134	76.0
C(13)-B(1)	0.146	-0.105	-0.229	-0.128	71.9
C(19)-B(1)	0.146	-0.107	-0.229	-0.128	72.0
F(1)···P(1)	0.018	0.063	-0.012	0.002	3.9
F(6)···P(1)	0.013	0.048	-0.009	0.002	2.8
F(6)···F(1)	0.006	0.026	-0.005	0.001	1.5
F(10)···F(5)	0.008	0.036	-0.006	0.002	1.9
F(10)···F(15)	0.011	0.059	-0.009	0.003	2.7
F(11)···H(6A)	0.008	0.030	-0.005	0.001	1.6
F(15)···H(9B)	0.008	0.034	-0.005	0.002	1.6
F(1)···H(6B)	0.009	0.037	-0.006	0.002	1.8
F(15)···C(8)	0.008	0.033	-0.005	0.001	1.7
C(19)···F(15)	0.010	0.044	-0.007	0.002	2.1
F(10)···C(30)	0.011	0.051	-0.008	0.002	2.5
C(13)···F(11)	0.012	0.051	-0.008	0.002	2.7
C(19)···H(9B)	0.004	0.014	-0.002	0.001	0.5

* Espinosa–Molins–Lecomte (EML) correlation [E. Espinosa, E. Molins, C. Lecomte, *Chem. Phys. Lett.* 1998, *285*, 170–173].

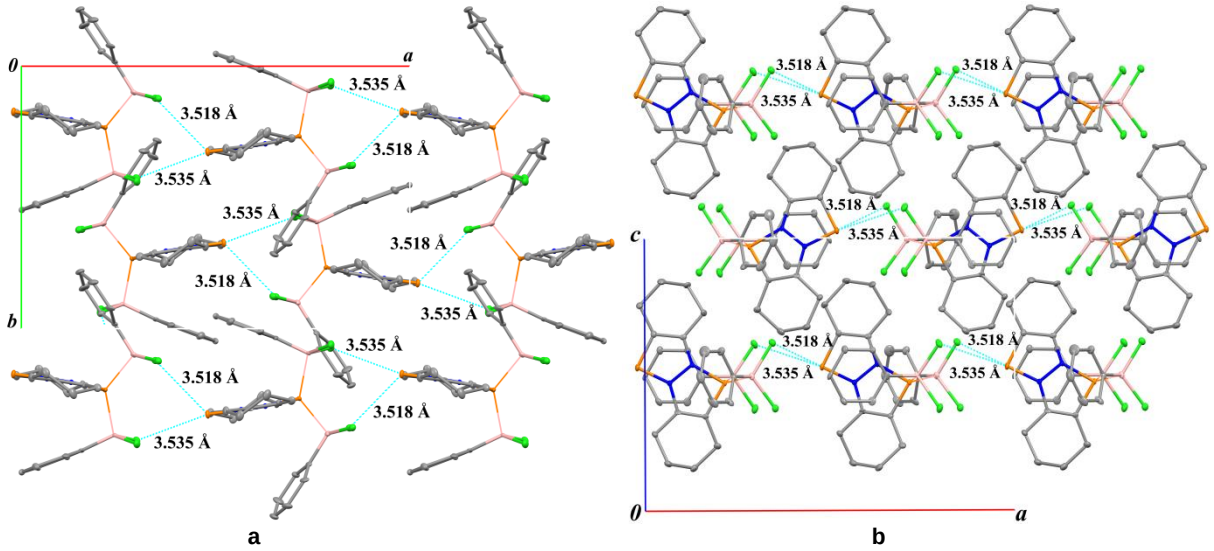

Figure S1. Fragment of crystal packing **14** along the crystallographic *c* (**a**) and *b* (**b**) axes. Hydrogen atoms are omitted for clarity.

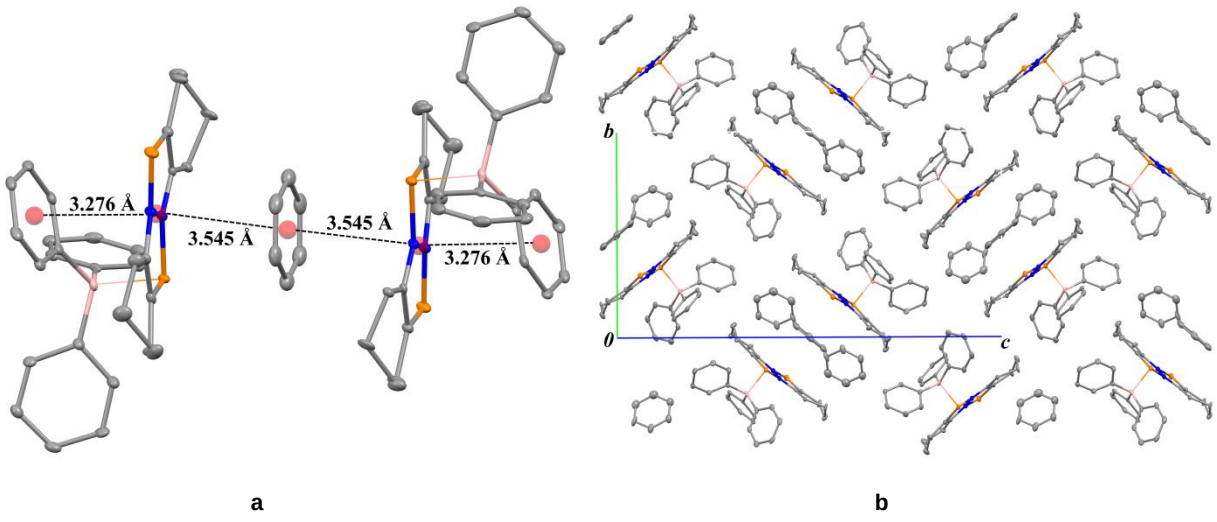

Figure S2. «Dimeric» motif (**a**) and the fragment of crystal packing **16** along the crystallographic *a* axis (**b**). Hydrogen and fluorine atoms are omitted for clarity. Red spheres indicate the centers of the phenyl rings and the centers of N-N bonds.

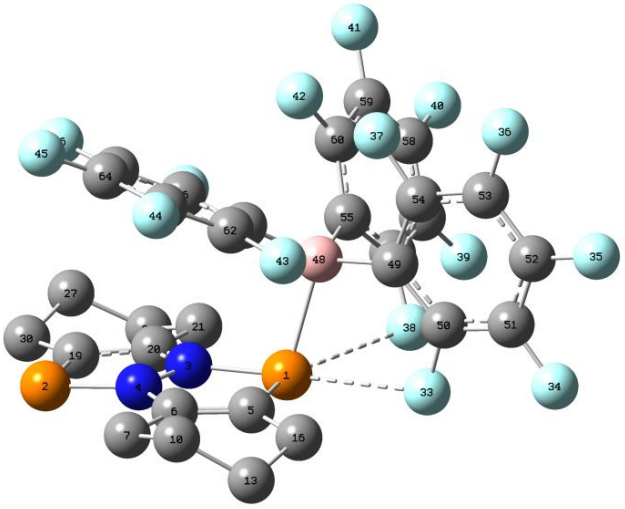

Figure S3. B3LYP/6-31G(d,p) optimized equilibrium geometries of **16**. Selected bond lengths [Å]: P(1)−B(48) 2.175, P(1)−F(33) 2.654, P(1)−F(38) 2.916, P(1)−N(3) 1.813, P(2)−N(4) 1.726, P(1)−C(5) 1.817, P(2)−C(19) 1.750.

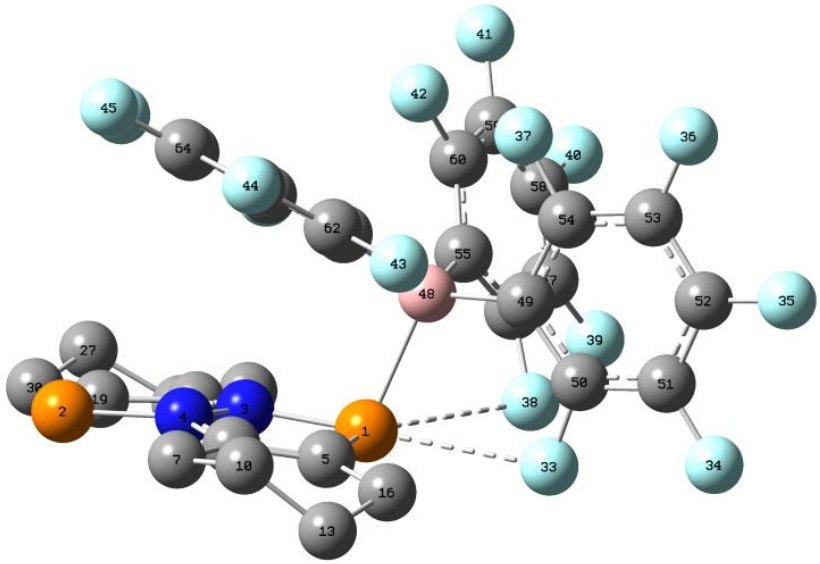

Figure S4. UB3LYP/6-31G(d,p) optimized equilibrium geometries of anion radical **16**$^{-\bullet}$. Selected bond lengths [Å]: P(1)−B(48) 2.147, P(1)−F(33) 2.775, P(1)−F(38) 3.004, P(1)−N(3) 1.791, P(2)−N(4) 1.774, P(1)−C(5) 1.830, P(2)−C(19) 1.792.

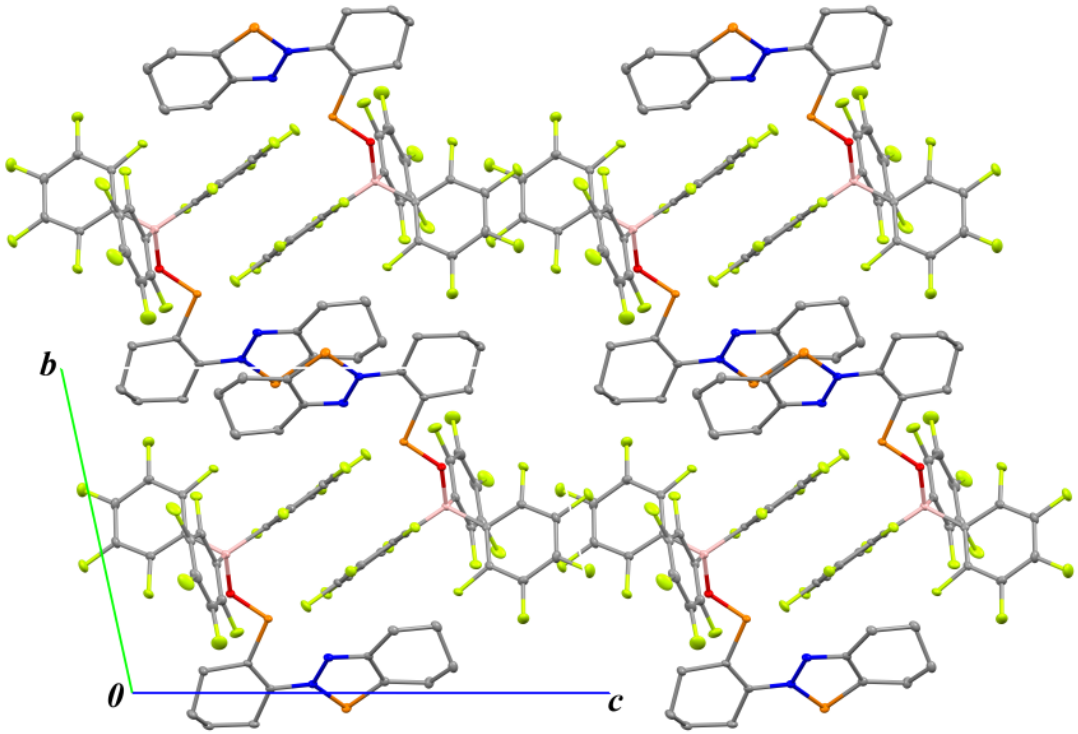

Figure S5. Fragment of crystal packing **17** along the crystallographic *a* axis. Hydrogen atoms and CH_2Cl_2 molecules are omitted for clarity.

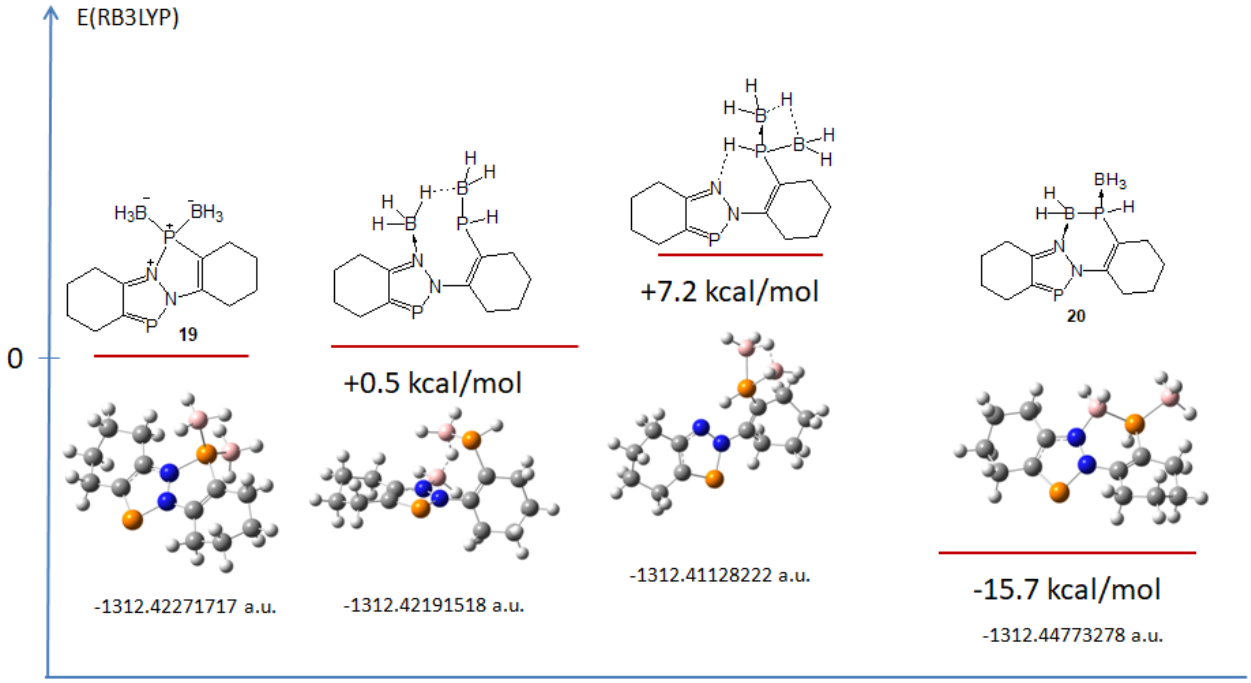

Scheme S1. B3LYP/6-31G(d) optimized equilibrium geometries of **19** and **20** and related intermediates with their total and relative energies.

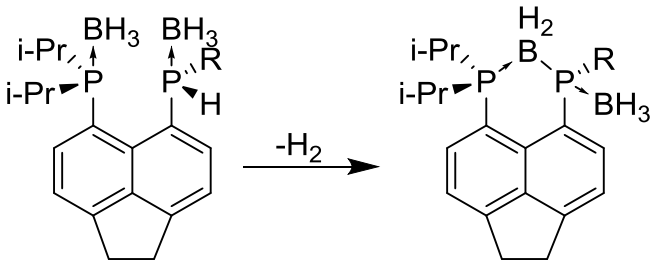

R = Ph, Fc, H

Scheme S2. Spontaneous dehydrocoupling in peri-substituted phosphine–borane adducts from ref. [L.J. Taylor, *Dalton Trans*. **2016**, *45*, 1976. DOI: 10.1039/c5dt02539g].

NMR spectra

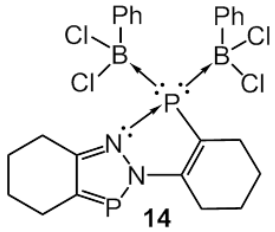

14

(^{1}H NMR, 200 MHz, 293 K, CD_2Cl_2)

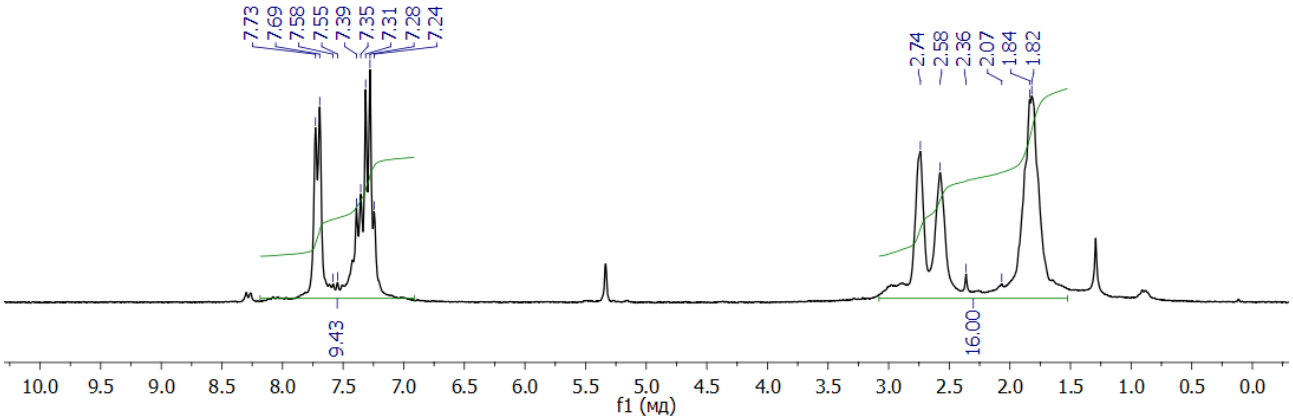

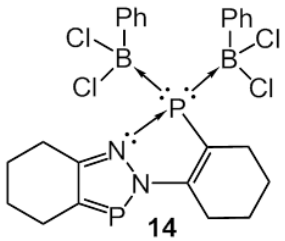

14

(^{1}H NMR, 400 MHz, 243 K, CD_2Cl_2)

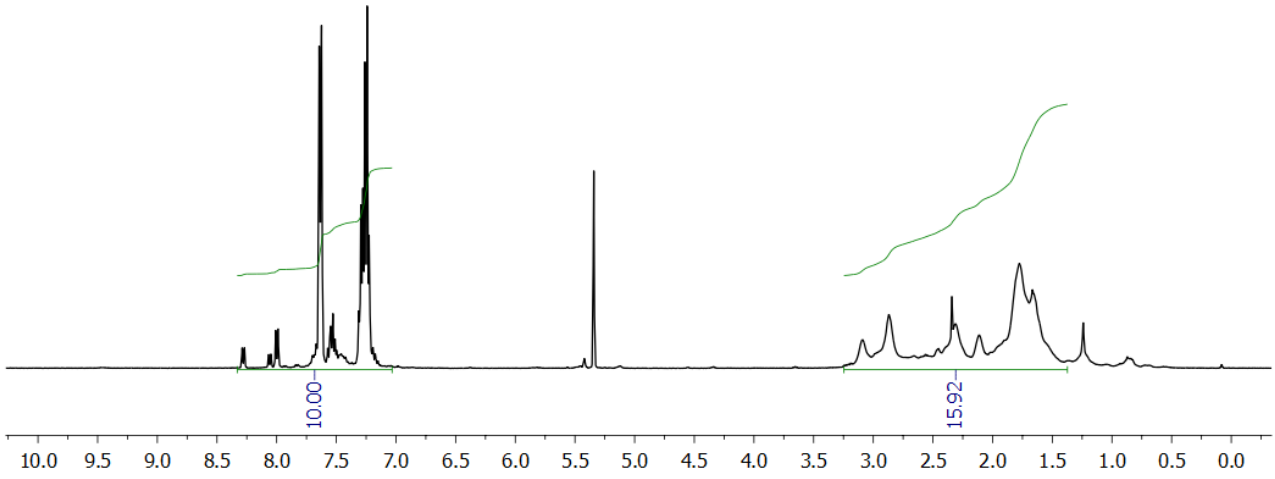

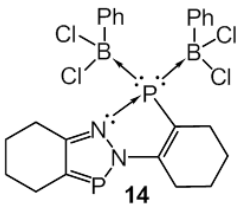

14

(^{31}P{^{1}H} NMR, 162 MHz, 293 K, CD_2Cl_2)

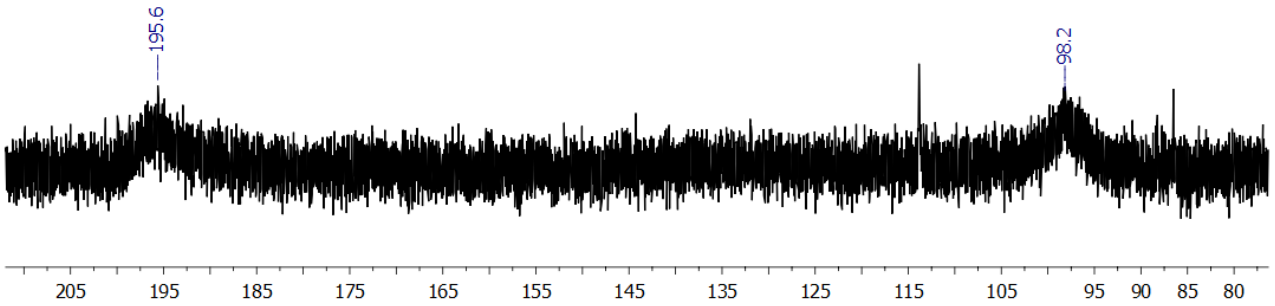

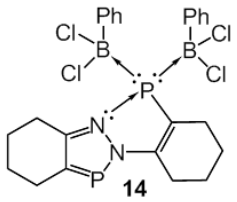

14

($^{31}P\{^{1}H\}$ NMR, 162 MHz, 233 K, CD_2Cl_2)

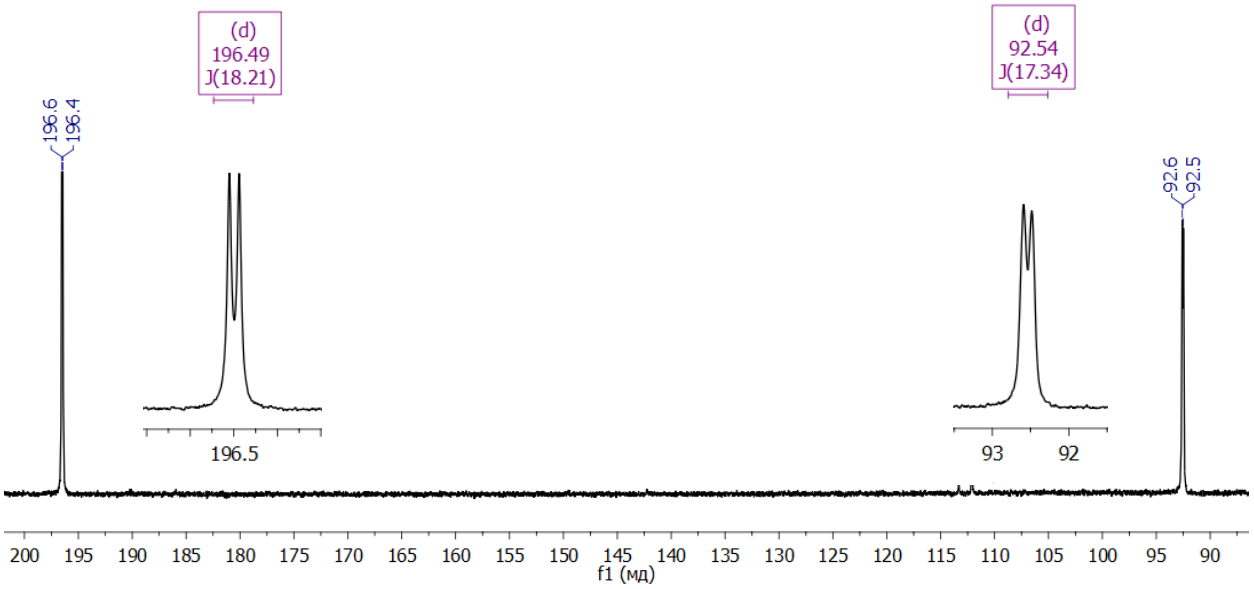

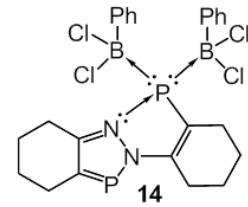

14

($^{11}B\{^{1}H\}$ NMR, 128 MHz, 293 K, CD_2Cl_2)

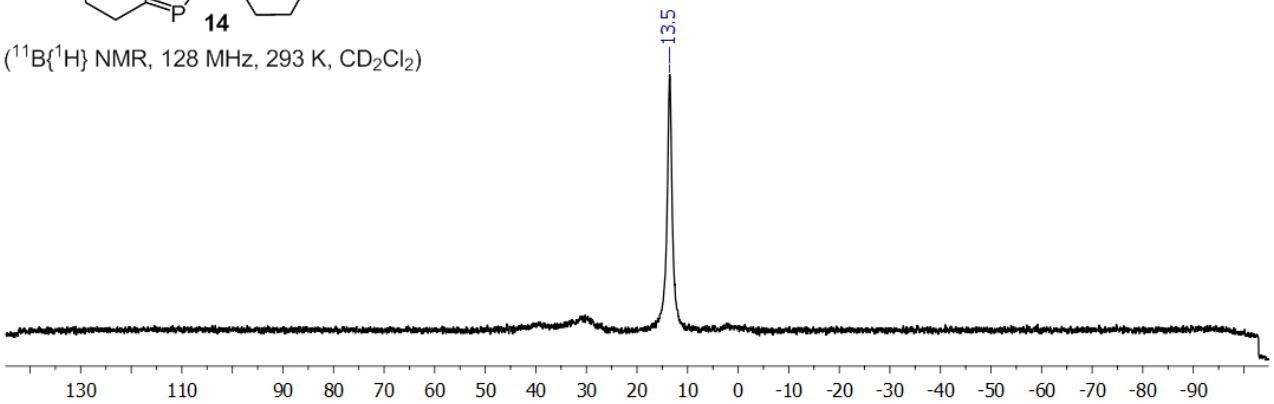

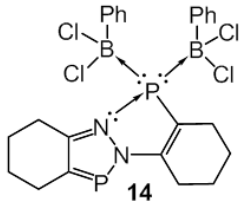

14

($^{11}B\{^1H\}$ NMR, 128 MHz, 233 K, CD_2Cl_2)

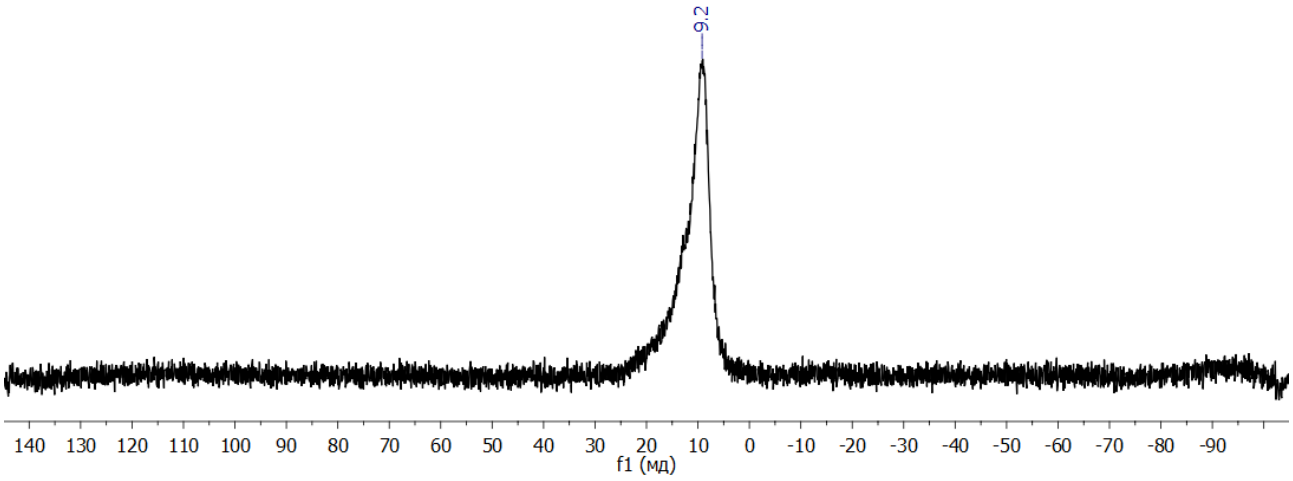

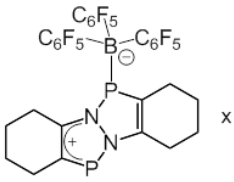

x $PhCH_3$ solvate

16

(^1H NMR, 400 MHz, 253 K, CD_2Cl_2)

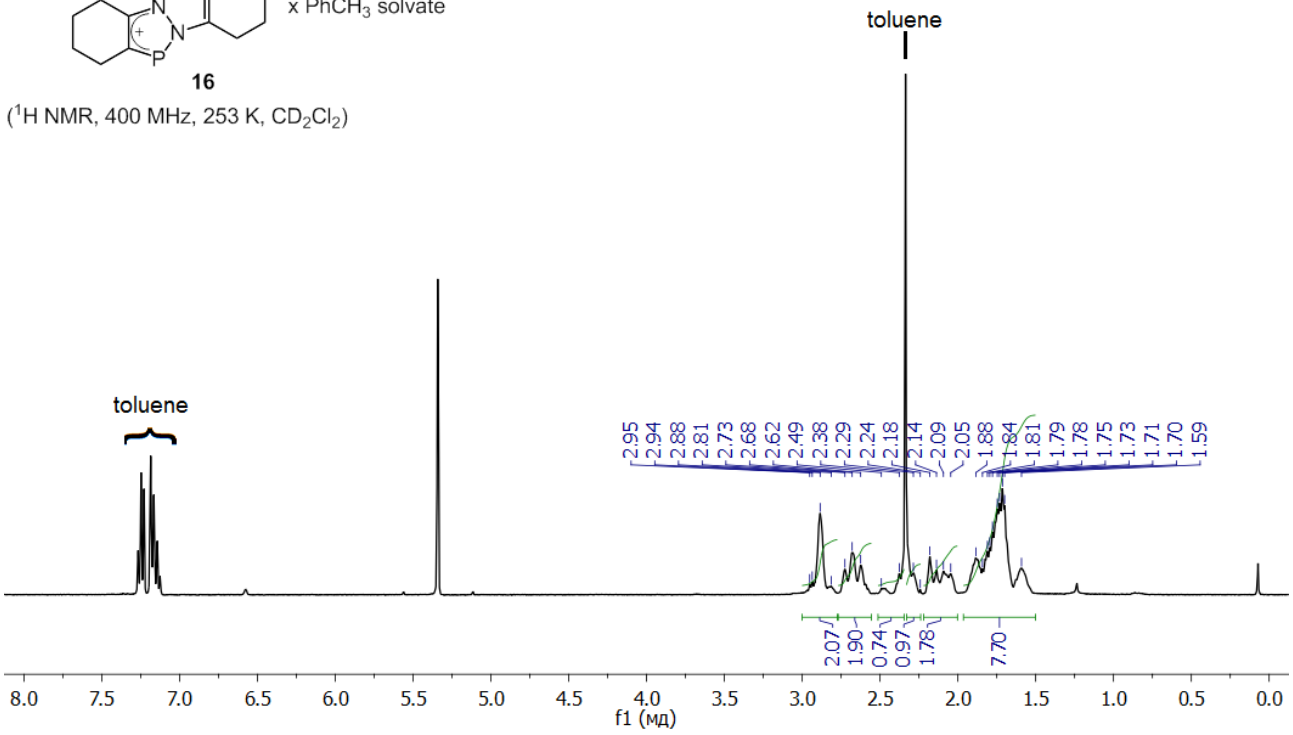

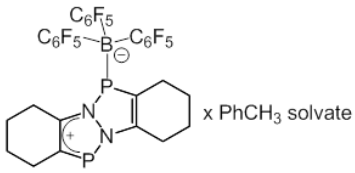

x $PhCH_3$ solvate

16

($^{13}C\{^1H\}$ NMR, 100 MHz, 298 K, CD_2Cl_2)

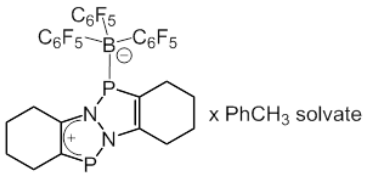

x $PhCH_3$ solvate

16

($^{31}P\{^1H\}$ NMR, 162 MHz, 233 K, CD_2Cl_2)

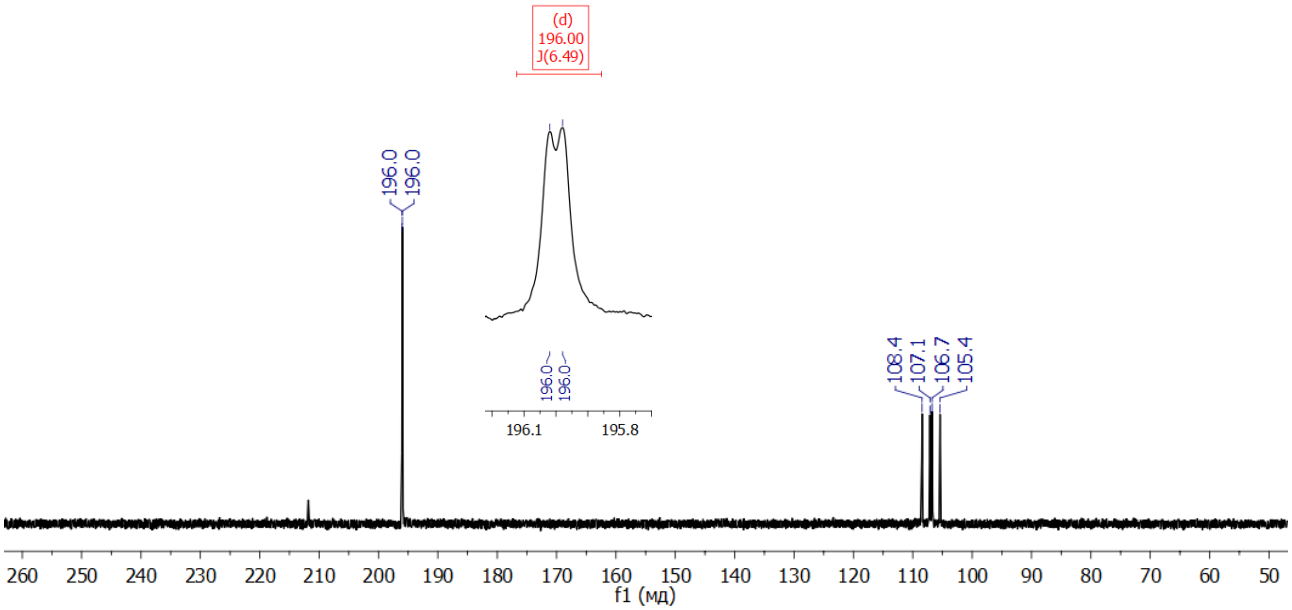

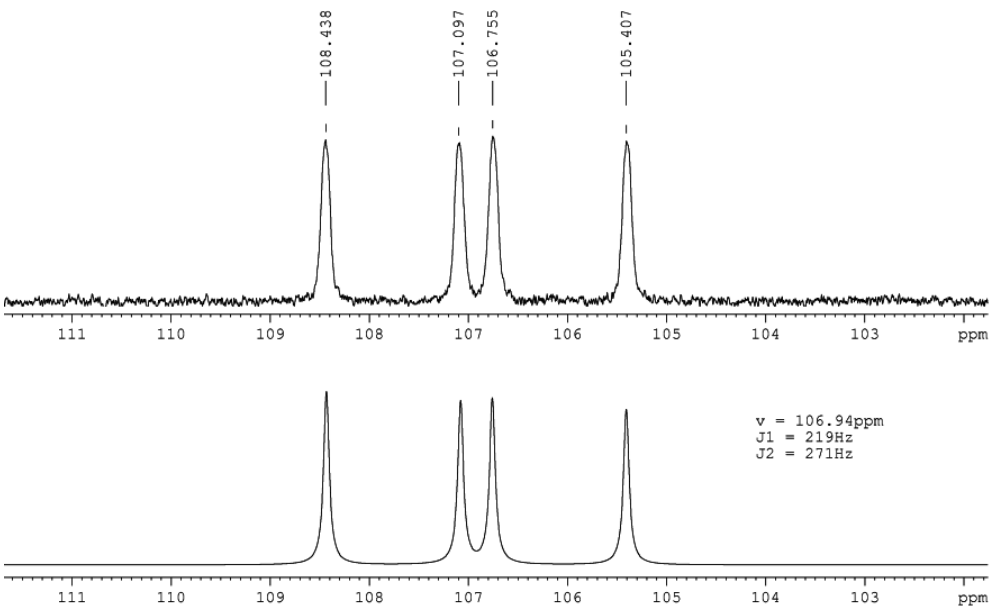

Fragment of the $^{31}P\{^{1}H\}$ NMR spectrum of compound **16** and simulated spectrum.

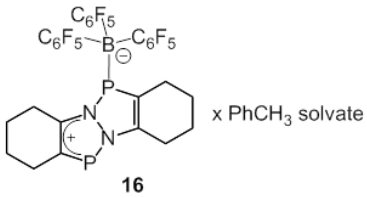

16

($^{11}B\{^{1}H\}$ NMR, 128 MHz, 253 K, CD_2Cl_2)

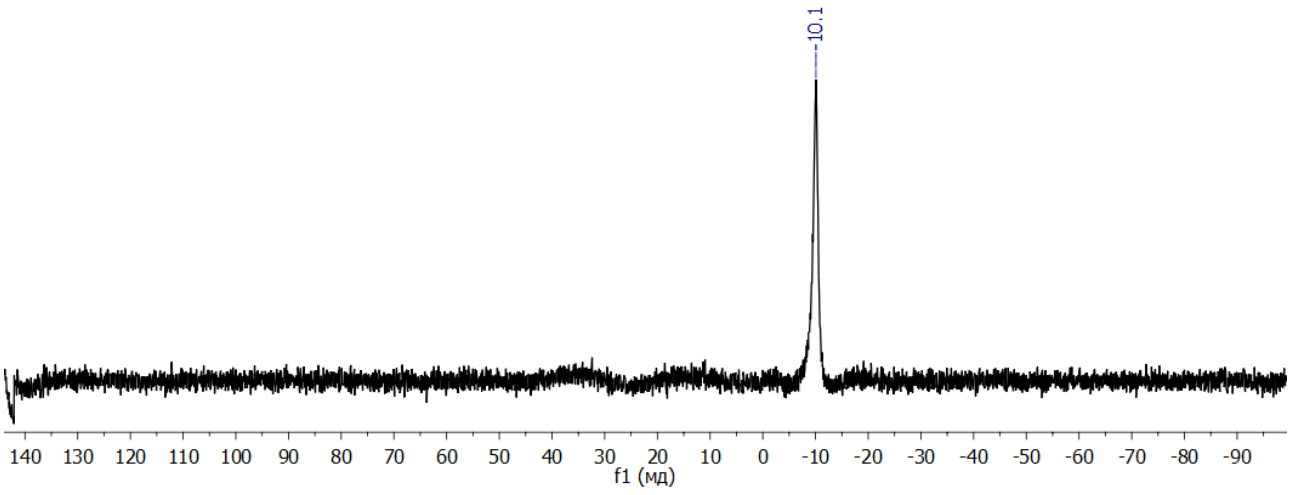

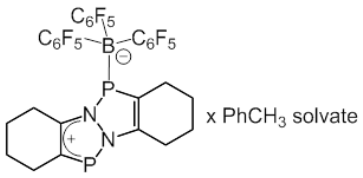

16

($^{19}F\{^{1}H\}$ NMR, 376 MHz, 253 K, CD_2Cl_2)

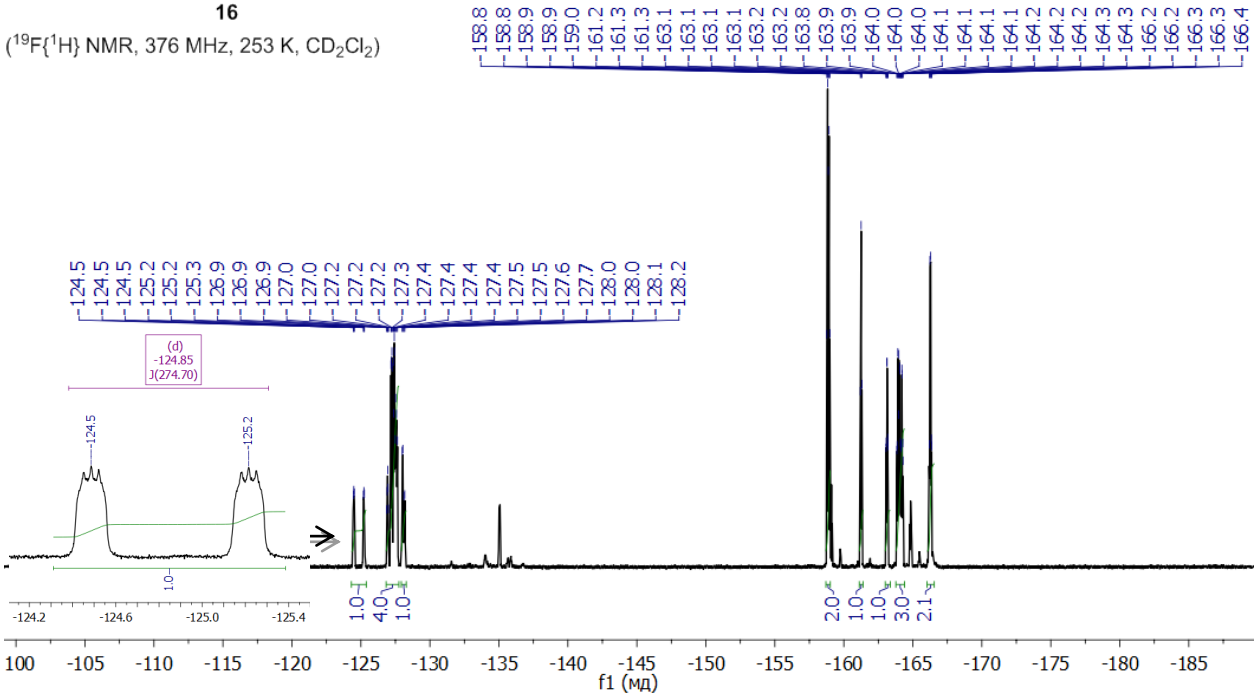

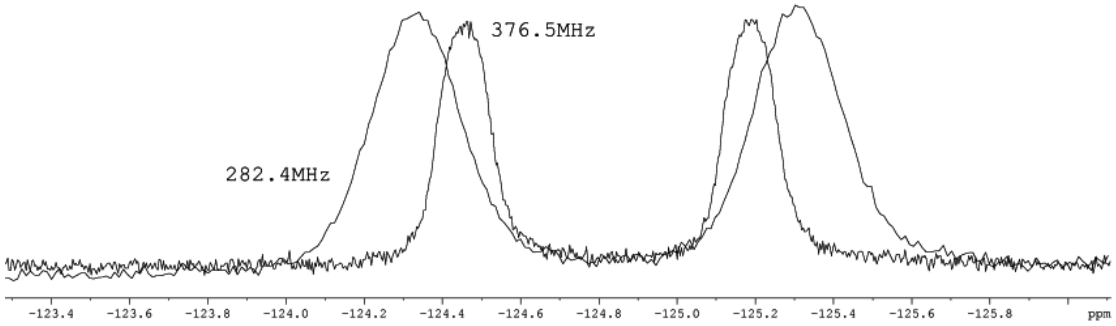

The fragment of ^{19}F NMR spectrum of compound **16** measured at 376.5 MHz (Bruker Avance 400) and 282.4 MHz (Bruker Avance 300) (293K) with the same ppm scale.

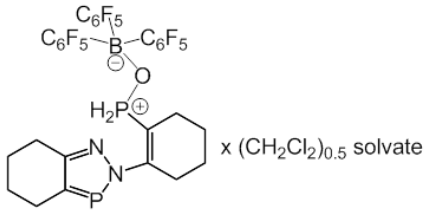

17

(^{1}H NMR, 400 MHz, 293 K, toluene-*d8*)

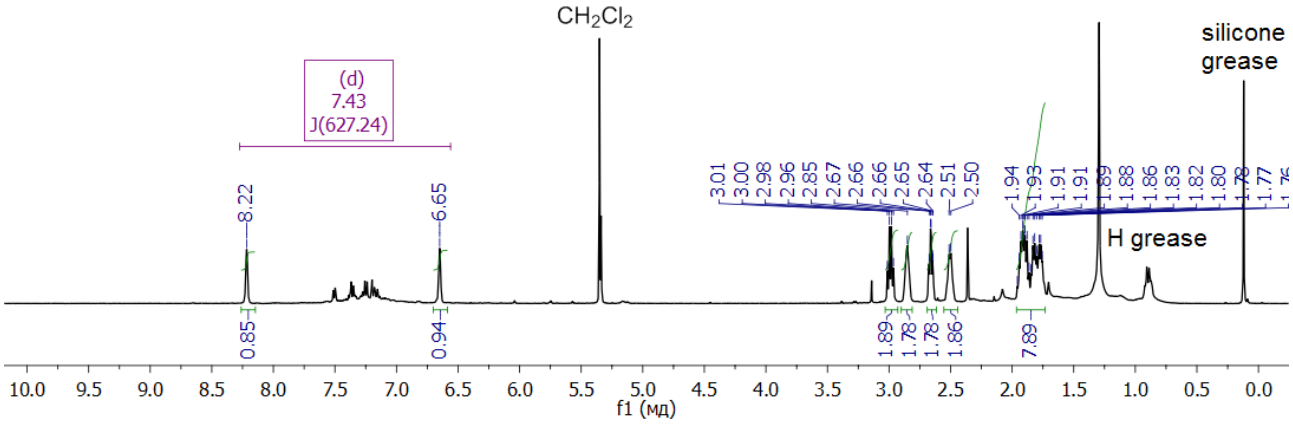

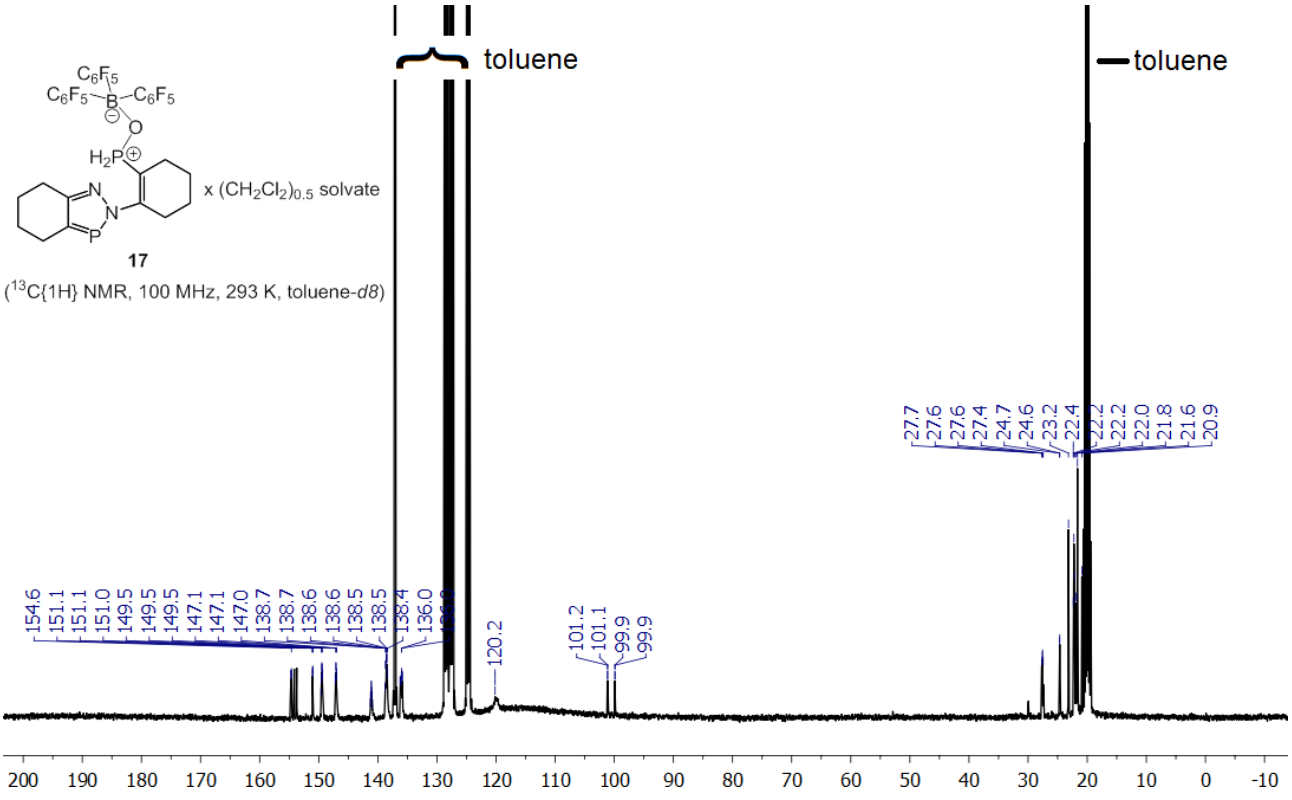

17

(^{13}C{1H} NMR, 100 MHz, 293 K, toluene-*d8*)

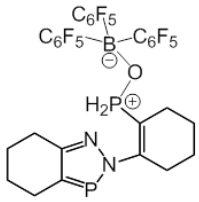

x $(CH_2Cl_2)_{0.5}$ solvate

17

($^{31}P\{^{1}H\}$ NMR, 162 MHz, 293 K, toluene-*d8*)

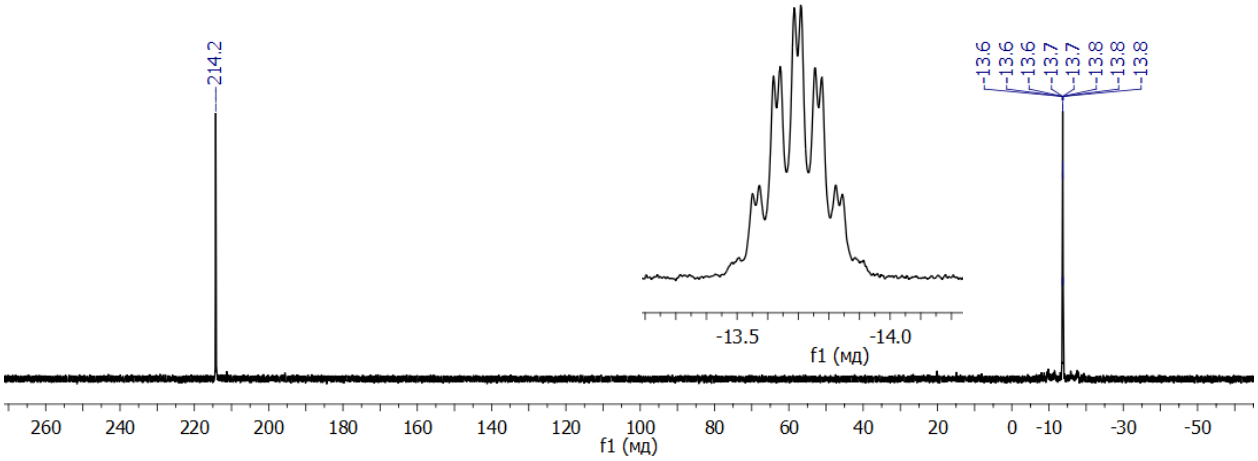

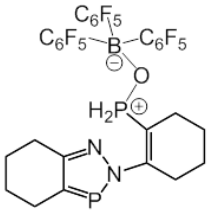

x $(CH_2Cl_2)_{0.5}$ solvate

17

(^{31}P NMR, 162 MHz, 293 K, toluene-*d8*)

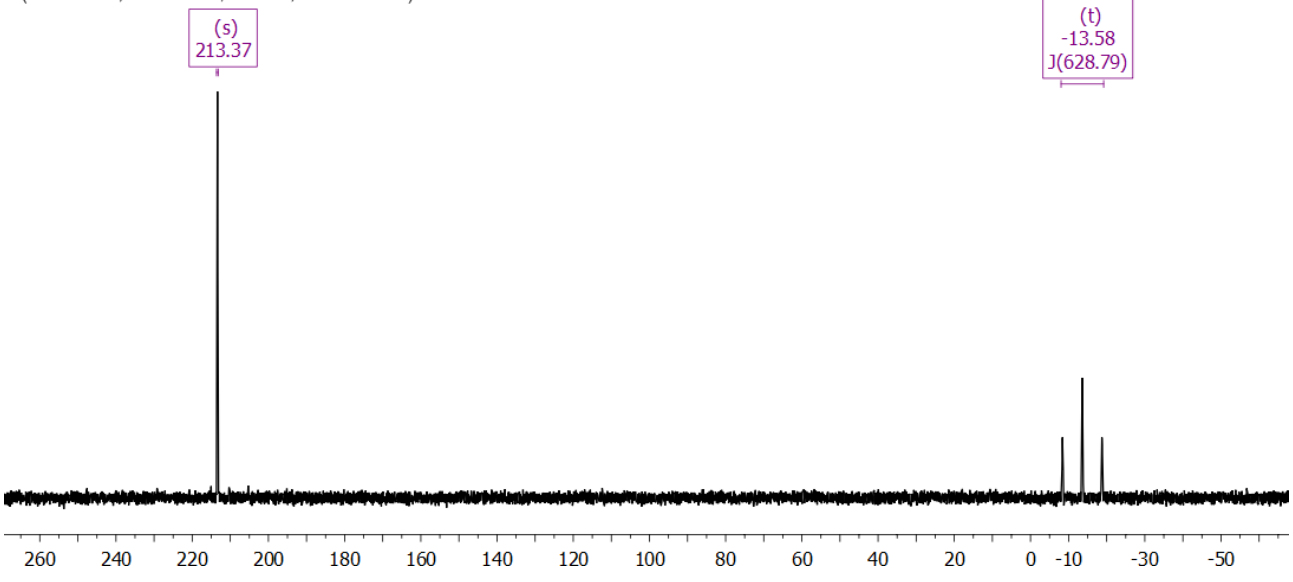

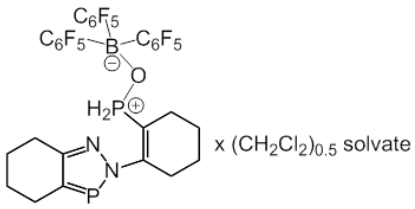

17

($^{11}B\{^1H\}$ NMR, 128 MHz, 293 K, toluene-*d8*)

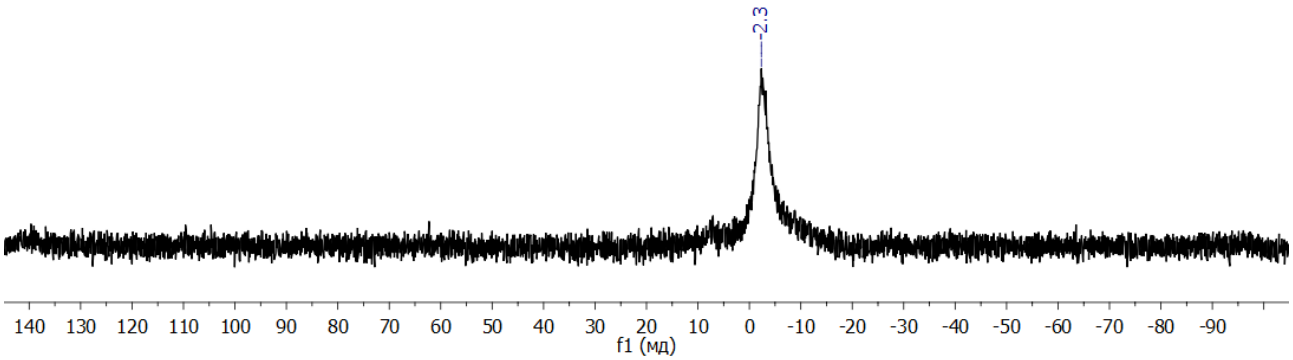

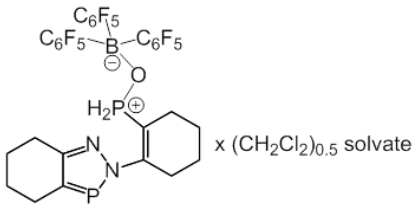

17

($^{19}F\{^1H\}$ NMR, 376 MHz, 293 K, toluene-*d8*)

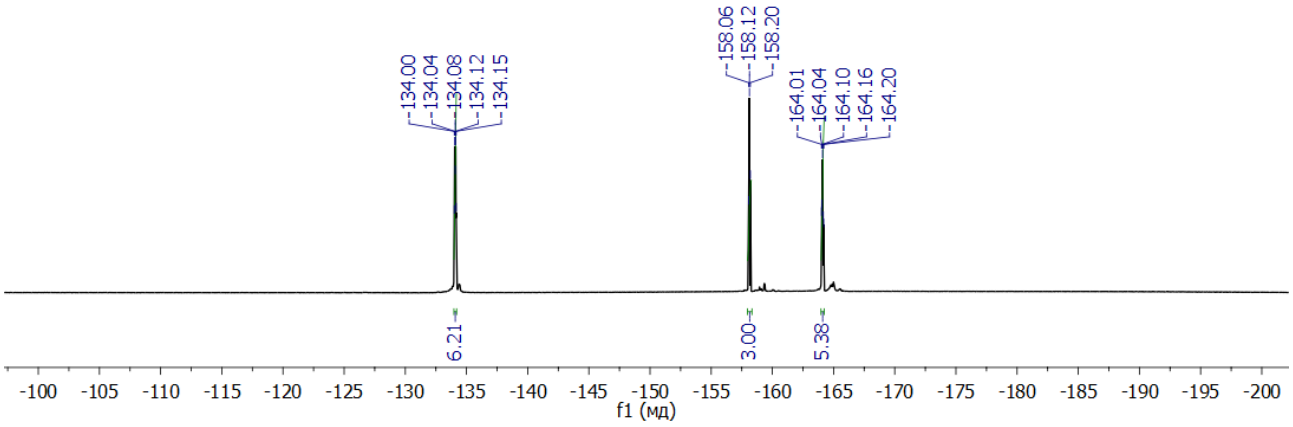

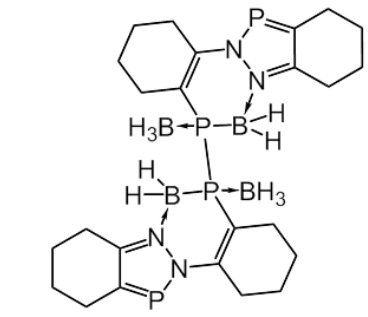

18

(^{1}H NMR, 400 MHz, 243 K, CD_2Cl_2)

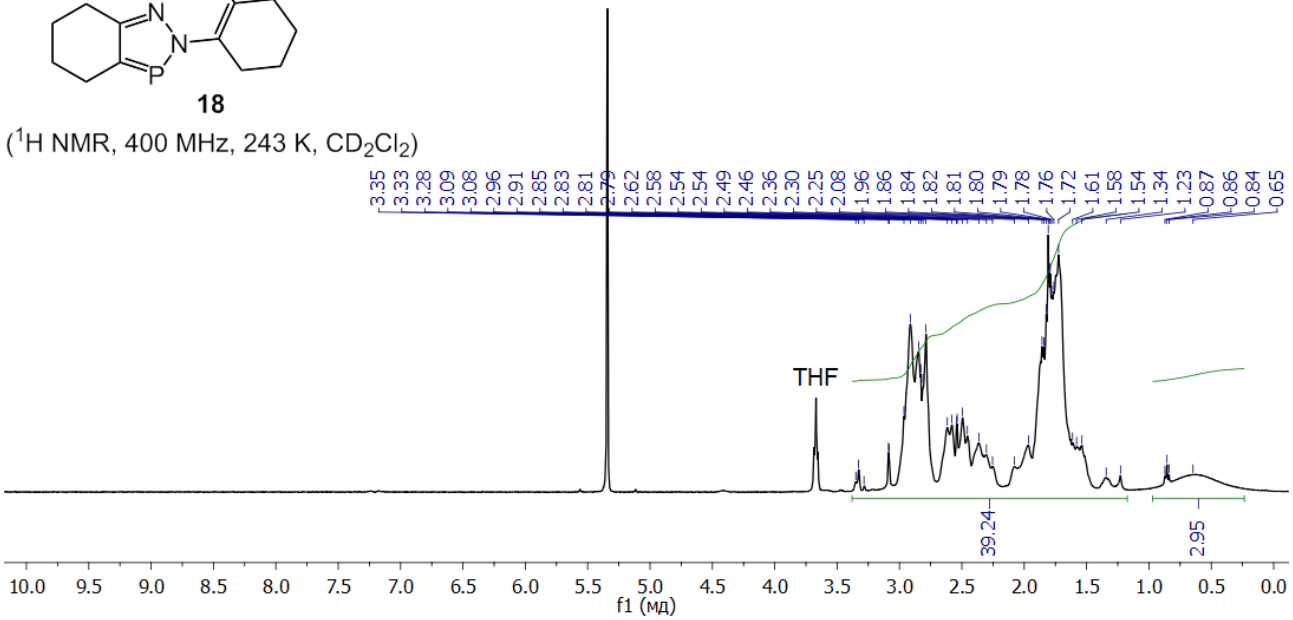

(^{31}P{^{1}H} NMR, 162 MHz, 243 K, CD_2Cl_2)

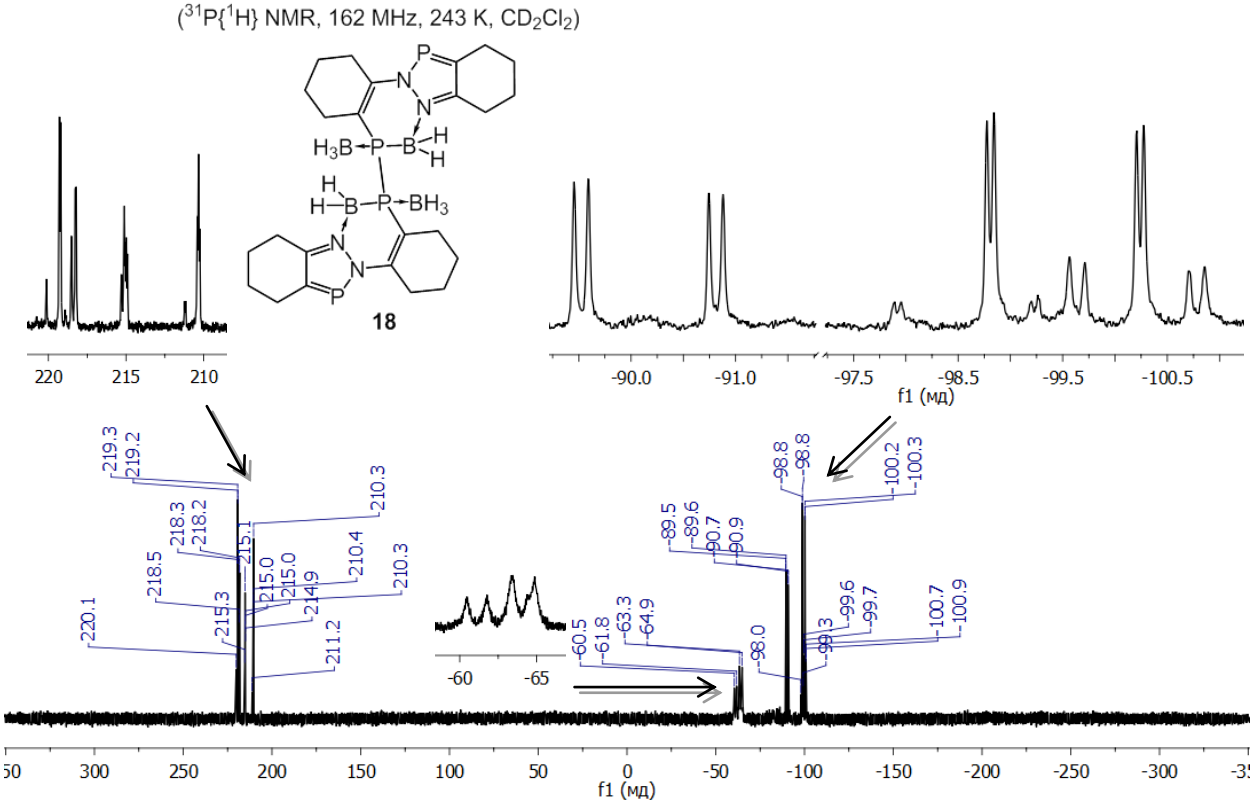

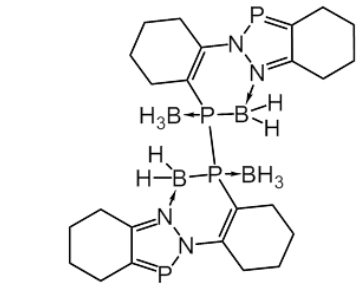

18

($^{11}B\{^{1}H\}$ NMR, 128 MHz, CD_2Cl_2)

green 293 K

purple 243 K